CIRP Annals - Manufacturing Technology xxx (2016) xxx–xxx

Contents lists available at ScienceDirect

CIRP Annals - Manufacturing Technology

journal homepage: http://ees.elsevier.com/cirp/default.asp

Error correction methodology for ultra-precision three-axis milling of freeform optics

J.D. Owen [a], J.A. Shultz [b], T.J. Suleski [b], M.A. Davies (1)[a,*]

[a] Center for Precision Metrology, Department of Mechanical Engineering and Engineering Science, University of North Carolina at Charlotte, Charlotte, NC, USA
[b] Center for Optoelectronics and Optical Communications, Department of Physics and Optical Sciences, University of North Carolina at Charlotte, Charlotte, NC, USA

ARTICLE INFO

Keywords:
Ultra-precision
Metrology
Freeform optics

ABSTRACT

Freeform optics facilitate a revolutionary approach to optical design. Ultra-precision diamond machining is an enabling technology for the manufacture of freeform optics. However, optical designs require tight tolerances across spatial wavelengths ranging from micro-roughness to overall form. To manufacture freeform optics to the necessary tolerances, a novel artifact-based error reduction methodology applicable to multi-axis diamond milling was developed. As demonstrated on a test sphere, the methodology reduces dominant error sources on the test sphere surface from 194 to 40 nm RMS. The approach is then successfully applied to an example freeform optical design where comparable error levels are achieved.

1. Introduction

Freeform optics allow great flexibility in the redirection of light in three dimensions, and thus open many new design degrees of freedom for the optical designer [1,2]. As defined by Fang et al. [3], a freeform optic has no axis of symmetry either on or off the part. Thus, the manufacturing methods for freeform optics must have three or more degrees-of-freedom. Ultraprecision machining is an enabling technology for freeform optics manufacture and includes coordinated-axis turning [4,5], flycutting [6], milling [7], and grinding [8]. However, the design tolerances on the optics are often very demanding. For example, for a specific visible light application – a glass freeform Alvarez lens [2] – the required surface micro-roughness is 1–2 nm RMS and the band-RMS tolerances from the mid-spatial frequencies (<1 mm spatial wavelength) to the form (>1 mm spatial wavelength) are in the range of tens of nm RMS. Meeting these tolerances requires better control and elimination of repeatable errors sources in the machining operations. Artifact-based methods for correcting errors in machining have been used for decades in the correction of tool errors in diamond turning [4,9]. Most diamond turning machines are also now equipped with on-machine error measurement and correction systems as suggested by Thompson et al. [10]. They measure part errors directly and produce compensated part programs, but these have not been applied to multi-axis milling.

This paper presents an artifact-based error correction methodology for three-axis ultraprecision milling that corrects for tool radius errors, decentering and tool waviness. The correction method requires the cutting and measurement of only two spherical artifacts: the first to construct the tool error model and the second to verify the model. Once the error model for the tool is constructed and verified, the model can be used for the cutting of an arbitrary freeform surface provided the tool set up, tool condition, and cutting conditions remain unchanged. The method also corrects synchronous dynamic motions of the milling tool due to imbalance and cutting forces that can be modeled as flute decentering. The algorithm for the error-corrected, tool-path generation approach is summarized and has been implemented in MATLAB®. The algorithm is demonstrated on an example freeform optical surface and resulting errors from the optical prescription are within the range desired for infrared and some visible light applications.

The novelty of the current research is: (1) the application of artifact-based error correction techniques to freeform diamond milling of optics; (2) the development of a tool-error model for a diamond endmill from a single spherical artifact, and (3) the implementation of the tool error model in a custom software code capable of correcting tool errors in the milling of an arbitrary freeform optical prescription. Further, because the error model is a property of the tool set-up, it is not necessary to make repeated, time-consuming measurements and corrections as with traditional on-machine correction techniques.

2. Experimental arrangement

All machining experiments were conducted on a Moore Nanotechnology 350 FG machine using three linear axes (*X*–*Y*–*Z*), a main spindle (C) with a maximum speed of 10,000 rpm and a milling spindle with a maximum speed of 60,000 rpm. The cutting parameters are the depth of cut a_p, the stepover b_r, the feed velocity vector $\mathbf{v_f}$, the feed per tooth f_z and the spindle speed n. The experimental arrangement and the main cutting parameters are

* Corresponding author.
E-mail address: madavies@uncc.edu (M.A. Davies).

http://dx.doi.org/10.1016/j.cirp.2017.04.031
0007-8506/© 2017 Published by Elsevier Ltd on behalf of CIRP.

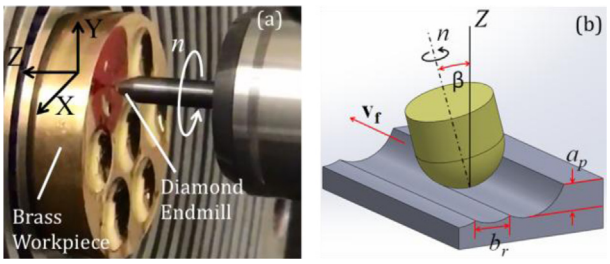

Fig. 1. Experimental arrangement: (a) photograph of freeform milling; and (b) cutting parameter definitions.

shown in Fig. 1. While the methodology is demonstrated here for three-axis milling, we do allow for a fixed tool inclination angle relative to the machine *Z*-axis, β. This can be resolved into components β_f and β_n. β_f is the inclination projected into the plane defined by the feed velocity $\mathbf{v_f}$ and machine *Z*-axis, and β_n is the inclination projected in to the plane perpendicular to the aforementioned plane. The nominal tool radius is R_k.

2.1. Cutting arrangement

A single crystal diamond, single-flute, ball-endmill with a nominal 1.5 mm radius and a zero-degree rake angle γ was used to machine brass C46400. The cutting arrangement is shown in Fig. 1. Milling cutting tests were done with n of 44,000 rpm. For rough and finish machining, rastering was done in the *y*-direction with an f_z of 9 μm and 1.4 μm respectively, a $\mathbf{v_f}$ of 400 mm/min and 60 mm/min, an a_P of 300 μm and 50 μm respectively, and b_r of 100 μm and 20 μm respectively. The inclination angle β was zero. No appreciable diamond wear has been seen previously in milling of brass C46400 and optical surface finish is readily achieved, making the material ideal for demonstration of this error correction methodology. The f_z, b_r, and the chord length in the feed direction were selected to produce an optical quality surface finish and were not affected by the correction method.

2.2. Dominant sources of error

In freeform milling of optics with a clear aperture on the order of tens of millimeters, it has been observed that tool errors dominate over repeatable machine errors and have a large effect on the errors in the machined optics. The dominant sources of tool error are shown in Fig. 2(a) for a single-flute, single crystal diamond, ball-endmill [11] and are similar to those seen in turning [9]. The errors are: (1) radial shift of the diamond relative to the axis of rotation (ε_r); (2) tool radius error ΔR_k; and (3) tool waviness $\varepsilon_w(\theta)$ as a function of nominal tool angle θ. The effect of ε_r on the form of a spherical artifact is shown in Fig. 2(b), and will be discussed further in Section 3.

2.3. Metrology equipment

Measurements of the artifacts were conducted on both a Form-Talysurf 120L and a Zygo Verifire interferometer. The Form-Talysurf 120L has a *z*-travel of 120 mm and a resolution of 10 nm. The resolution of the Zygo Verifire is approximately 0.5 nm.

3. Machine path planning and error correction methodology

3.1. Definition of optical prescription

Typically, a freeform optic is defined by an optical prescription in either polar $z = g(\rho,\theta)$ or Cartesian coordinates $z = f(x,y)$, potentially containing an asphere equation, sums of functional basis sets such as Zernike polynomials, or combinations thereof. Generation of the tool path at the level required by optical designs may require the development of a custom tool path generator (e.g. [5]) as commercially available CAM software may not have the necessary fidelity. We have developed a custom tool path generator in MATLAB®, and this tool path generator is readily integrated with the tool error model as described below.

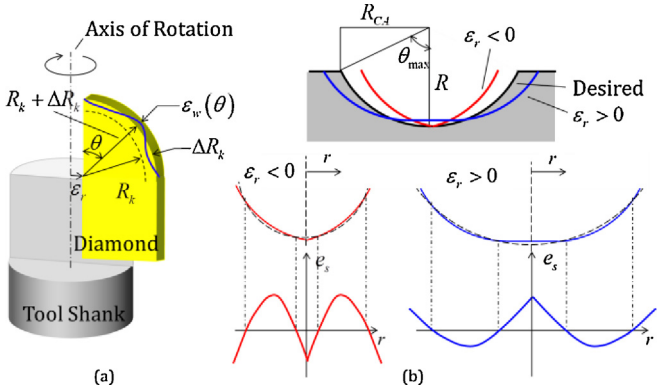

Fig. 2. (a) Dominant error sources associated with the tool and (b) the effect of radial offset ε_r on deviation from best sphere (dotted lines) for a spherical artifact when $\varepsilon_r > 0$ (blue) and $\varepsilon_r < 0$ (red).

3.2. Artifact-based tool-error model development

A tool error model encompassing the main repeatable error sources identified in Fig. 2(a) must be developed. A spherical artifact is sufficient to identify the dominant tool errors ε_r, ΔR_k and $\varepsilon_w(\theta)$ that comprise the tool error model. To determine the tool error model, a suitable spherical artifact is designed to match the final applications. As shown in Fig. 2(b), the sphere radius R and clear aperture radius R_{CA} must sample as much of the tool edge (θ_{max}) as is required to cut the desired freeform optics.

As shown in Fig. 2(b), the effect of ε_r on the spherical artifact is to either compress ($\varepsilon_r < 0$, red) or expand ($\varepsilon_r > 0$, blue) the clear aperture of the artifact and makes it non-spherical (i.e. ogive error [9]). When the artifact is measured and compared to a best fit sphere, the error, $e = z_m - z_s$, is equal to the difference between the height of the measured surface (z_m) and the best fit sphere (z_s). The error, *e*, takes on a characteristic "M" or "W" shape for positive and negative ε_r, respectively. The procedure for estimating ε_r is demonstrated in Fig. 3. A shift, ε_s, at the data center ($r = 0$) is introduced to the measured artifact data, z_m. Then, the shifted data is fit with a new best fit sphere to obtain a new z_s, and this procedure is continued until the error *e* is minimized; here we use the peak-to-valley as a measure to minimize *e*, denoted $e_{p\text{-}v}$. The optimum value ε_{so} that minimizes $e_{p\text{-}v}$ provides an estimate of the tool error $\varepsilon_r = -\varepsilon_{so}$. For a tool having only ε_r, the minimum $e_{p\text{-}v}$ will be zero. In practice, the minimum error will still include tool waviness and other errors and will be non-zero. Further, when the

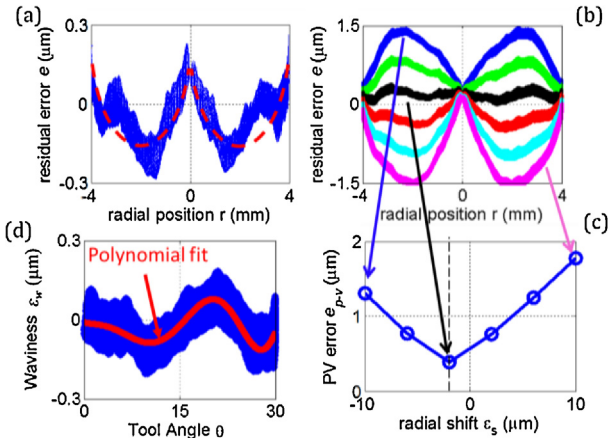

Fig. 3. Determining ε_r by minimizing $e_{p\text{-}v}$ where: (a) shows radial cross sections of *e* from an interferometric map of the errors; (b) shows the introduction of a shift and the effect on the shape; (c) shows the evolution of $e_{p\text{-}v}$ with ε_s; and (d) shows residual tool waviness $\varepsilon_w(\theta)$.

Please cite this article in press as: Owen JD, et al. Error correction methodology for ultra-precision three-axis milling of freeform optics. CIRP Annals - Manufacturing Technology (2017), http://dx.doi.org/10.1016/j.cirp.2017.04.031